JOURNAL OF GUIDANCE, CONTROL, AND DYNAMICS
Vol. 21, No. 4, July–August 1998

Application of Singular Value Decomposition Method to Digitally Controlled Large Orbiting Platforms

Aprille J. Ericsson-Jackson,* Peter M. Bainum,† and Guangqian Xing‡
Howard University, Washington, D.C. 20059

The dynamics and control for the specific application of a large orbiting flexible thin square plate are considered. The focus is on the utilization of a singular value decomposition (SVD) method to create a stable reduced-order system. By reviewing the system's singular value bounds in the frequency domain one can properly assess stability robustness parameters that are difficult to characterize effectively in a time-domain setting. This system's open-loop singular values were extremely close to zero, denoting singular system matrices. To alleviate this problem with matrix singularity, the SVD method was applied to transform the original systems. The reduction of actuators/sensors is done partially in the physical sense and partially in the mathematical space. Results show that when the SVD method transformation is applied stable controllable closed-loop system matrices can be designed.

Introduction

LARGE space structures are typically highly flexible and usually are represented by systems of ordinary differential equations with many degrees of freedom. Because the structure may have a large number of significant elastic modes, its mathematical model has a high order. However, to reduce the on-line control computation time it is necessary to design a controller/estimator based on a reduced-order system model.

The present paper considers the dynamics and control for the specific application of a large, orbiting, flexible, thin square plate. This work will focus on the utilization of a singular value decomposition (SVD) method to create a stable reduced-order system.

By reviewing the system's open-loop singular value bounds (the bounds are the difference between the minimum and maximum singular value) in the frequency domain, one can properly assess stability robustness parameters that are difficult to characterize effectively in a time-domain setting. Through the comparison of the singular values of the system transfer function, one arrives at suitable ranges for stability robustness. Singular value plots are utilized for analysis of the various systems throughout this research. It was noted that the system's open-loop singular values were extremely close to zero, denoting a lack of linear independence in some of the system matrices. To alleviate this problem with singularity, the SVD method was applied to transform the original systems to a linearly independent controller/observer system. Results show when the SVD method is applied, a transformation occurs to system matrices, which helps to diminish the approach of the system toward singularity.

Methodology

The plate's dynamic equations of motion are developed by applying a Eulerian–Newtonian approach named Santini's[1] formulation. These equations are linearized and placed in a state-space matrix format.[2] An application of finite element method algorithms, NASTRAN,[3] provides the system flexible modes and modal patterns for modeling of the system.

Attitude and shape control are achieved by placing point thrusters on the surface of the plate.[4] It is assumed that for measuring the attitude and displacement of the deformed plate that two Earth horizon sensors, two sun sensors and between 6 and 12 displacement sensors are to be employed. The displacement sensors are assumed to be collocated with the point thrusters located on the major surface of the plate; these collocated actuator and sensor positions are verified for controllability and observability. The concepts of degree of controllability/observability are applied to the actuator/sensor placement problem.[5,6]

The theory of multi-input/multi-output is applied to the system transfer function matrix in the Z domain for the analysis and design of robust control of multivariable discrete-time feedback systems in the frequency domain.[7] Application of the linear quadratic regulator and linear quadratic Gaussian (LQG) theory with Kalman filtering provides the control law feedback and estimator/filter gains, respectively. These gain matrices are utilized for studying the robustness recovery properties of the integrated LQG/loop transfer recovery designed control system.[8] The SVD[9] method is applied in the robust eigenstructure assignment providing a measurement of the system singularity and stability performance margins. Simultaneously, nonlinear and sequential linear programming algorithms are applied for the optimization of the system controller design. Specifically, implementation of the MATLAB routines enable analysis of the system robustness in the discrete-time and frequency domains.[10]

Assumptions

This paper assumes the platform structure is a thin plate; this allows for the application of the first-order plate-bending theory, which ensures that internal strains are within the linear range. The structure is modeled as a large, thin square flexible orbiting plate traveling at a constant angular rate around the Earth. For many space applications it is required that the major surface of the plate be pointed toward the Earth; therefore, this orientation was selected. The structure is made of composite graphite/epoxy. Because, normally, only a few elastic modes contribute significantly to the vibrational motion of the structure, initially, the first six elastic modes are considered in the system model; then the number of state variables are reduced to contain only the first three elastic modes. The system is transformed to the discrete-time domain.

Several possible arrangements for actuator/sensor placement are considered in this investigation (Fig. 1). Each arrangement employs between 6 and 12 actuators/sensors placed along the outer edge of the platform (unprimed) and within the boundary of the platform (primed). A majority of the actuators/sensors are assumed to exert/detect forces normal to the major surface; they help control/monitor the shape deformation and also provide/sense the torque about the two major axes in the plane of the plate. The other actuators/sensors (5 and 6 and 11 and 12) are placed along the edge of the plate; they provide control and monitoring for the torque about the third axis, normal to the major surface.

The maximum order of the open-loop state vector is selected to be 18. The state includes three rigid rotational modes plus six flexible transverse modes. (Yu[11] has shown that coupling between

Presented as Paper AAS 97-722 at the AAS/AIAA Astrodynamics Conference, Sun Valley, ID, Aug. 4–7, 1997; received Aug. 29, 1997; revision received Jan. 10, 1998; accepted for publication Jan. 11, 1998. Copyright © 1998 by the American Institute of Aeronautics and Astronautics, Inc. All rights reserved.

*Graduate Research Assistant, Department of Mechanical Engineering; currently Aerospace Engineer, NASA Goddard Space Flight Center, Greenbelt, MD 20771. Member AIAA.

†Distinguished Professor of Aerospace Engineering, Department of Mechanical Engineering. Fellow AIAA.

‡Senior Research Associate, Department of Mechanical Engineering.

Table 1 Systems analyzed

System	Description of states	Actuator/sensor placement	Order of state n	Number of sensors (full/reduced) m	Number of actuators (full/reduced) r
1	3 rigid + 6 modes	Outer	18	16/8	12/8
2	3 rigid + 6 modes	Inner	18	16/8	12/8
3	3 rigid + 3 modes	Outer	12	10/6	6/6
4	3 rigid + 3 modes	Inner	12	10/6	6/6
5	3 rigid + 2 modes	Outer	10	10/5	10/5
6	3 rigid + 6 modes	Inner/outer	18	16/9	12/9

translational and rigid rotational motions is very small. If the translational modes are needed they can be obtained through a transformation from the flexible modes.) With this background six different systems are analyzed in this paper, as described in Table 1. Systems 3 and 4 represent a reduction in the number of states in the model, as well as a reduction in the number of actuators and sensors.

State-Space Formulation

The general state-space equation is defined as[2]

$$\{\dot{X}\} = [A]\{X\} + [B]\{U\} \tag{1}$$

where the state vector $\{X\}$ is

$$\begin{aligned} &\psi = x_1, \quad \psi' = \frac{d\psi}{d\tau} = x_2, \quad \theta = x_3, \quad \theta' = x_4 \\ &\phi = x_5, \quad \phi' = x_6 \\ &Z_1 = x_7, \quad Z_1' = x_8, \quad Z_2 = x_9, \quad Z_2' = x_{10}, \ldots \\ &Z_6 = x_{17}, \quad Z_6' = x_{18} \end{aligned} \tag{2}$$

and the state matrix $[A]$ is

$$[A] = \begin{bmatrix} 0 & 1 & 0 & 0 & 0 & 0 & 0 & 0 & 0 & \cdots & 0 & 0 & 0 \\ \Omega_x & 0 & 0 & 0 & 0 & (1+\Omega_X) & 0 & 0 & 0 & \cdots & \vdots & \cdot & \vdots \\ 0 & 0 & 0 & 1 & 0 & 0 & 0 & 0 & 0 & \cdots & \cdot & \vdots & \cdot \\ 0 & 0 & 3\Omega_y & 0 & 0 & 0 & 0 & 0 & 0 & \cdots & \vdots & \cdot & \vdots \\ 0 & 0 & 0 & 0 & 0 & 1 & 0 & 0 & 0 & \cdots & \cdot & \vdots & \cdot \\ 0 & (\Omega_z - 1) & 0 & 0 & -4\Omega_z & 0 & 0 & 0 & 0 & \cdots & \vdots & \cdot & \vdots \\ 0 & 0 & 0 & 0 & 0 & 0 & 0 & 1 & \vdots & \cdots & \cdot & \vdots & \cdot \\ 0 & 0 & 0 & 0 & 0 & 0 & 3-(\omega_1/\omega_c)^2 & 0 & 0 & \cdots & \vdots & \cdot & \vdots \\ 0 & 0 & 0 & 0 & 0 & 0 & 0 & 0 & 0 & 1 & \cdot & \vdots & \cdot \\ 0 & 0 & 0 & 0 & 0 & 0 & 0 & 0 & 3-(\omega_2/\omega_c)^2 & 0 & 0 & \cdot & \vdots \\ 0 & 0 & 0 & 0 & 0 & 0 & 0 & 0 & 0 & \vdots & 0 & \vdots & 0 \\ 0 & 0 & 0 & 0 & 0 & 0 & 0 & 0 & 0 & 0 & \vdots & 0 & 1 \\ 0 & 0 & 0 & 0 & 0 & 0 & 0 & 0 & 0 & 0 & 0 & 3-(\omega_6/\omega_c)^2 & 0 \end{bmatrix} \tag{3}$$

The control matrix is represented as

$$[B]\{U\} = \begin{bmatrix} 0 & 0 & 0 & 0 & 0 & 0 & 0 & 0 & 0 & 0 & 0 & 0 \\ 0 & 0 & 0 & 0 & \frac{y}{I_x} & \frac{y}{I_x} & 0 & 0 & 0 & 0 & \frac{-z}{I_x} & \frac{-z}{I_x} \\ 0 & 0 & 0 & 0 & 0 & 0 & 0 & 0 & 0 & 0 & 0 & 0 \\ \frac{z}{I_y} & \frac{z}{I_y} & \frac{z}{I_y} & \frac{z}{I_y} & 0 & 0 & \frac{z}{I_y} & \frac{z}{I_y} & \frac{z}{I_y} & \frac{z}{I_y} & 0 & 0 \\ 0 & 0 & 0 & 0 & 0 & 0 & 0 & 0 & 0 & 0 & 0 & 0 \\ \frac{-y}{I_z} & \frac{-y}{I_z} & \frac{-y}{I_z} & \frac{-y}{I_z} & 0 & 0 & \frac{-y}{I_z} & \frac{-y}{I_z} & \frac{-y}{I_z} & \frac{-y}{I_z} & 0 & 0 \\ 0 & 0 & 0 & 0 & 0 & 0 & 0 & 0 & 0 & 0 & 0 & 0 \\ \frac{\pm\Phi_{x1}^{(1)}}{M_1\ell\omega_c^2} & \frac{\pm\Phi_{x2}^{(1)}}{M_1\ell\omega_c^2} & \frac{\pm\Phi_{x3}^{(1)}}{M_1\ell\omega_c^2} & \frac{\pm\Phi_{x4}^{(1)}}{M_1\ell\omega_c^2} & 0 & 0 & \frac{\pm\Phi_{x7}^{(1)}}{M_1\ell\omega_c^2} & \frac{\pm\Phi_{x8}^{(1)}}{M_1\ell\omega_c^2} & \frac{\pm\Phi_{x9}^{(1)}}{M_1\ell\omega_c^2} & \frac{\pm\Phi_{x10}^{(1)}}{M_1\ell\omega_c^2} & 0 & 0 \\ 0 & 0 & 0 & 0 & 0 & 0 & 0 & 0 & 0 & 0 & 0 & 0 \\ \frac{\pm\Phi_{x1}^{(2)}}{M_2\ell\omega_c^2} & \frac{\pm\Phi_{x2}^{(2)}}{M_2\ell\omega_c^2} & \frac{\pm\Phi_{x3}^{(2)}}{M_2\ell\omega_c^2} & \frac{\pm\Phi_{x4}^{(2)}}{M_2\ell\omega_c^2} & 0 & 0 & \frac{\pm\Phi_{x7}^{(2)}}{M_2\ell\omega_c^2} & \frac{\pm\Phi_{x8}^{(2)}}{M_2\ell\omega_c^2} & \frac{\pm\Phi_{x9}^{(2)}}{M_2\ell\omega_c^2} & \frac{\pm\Phi_{x10}^{(2)}}{M_2\ell\omega_c^2} & 0 & 0 \\ \vdots & \vdots & \vdots & \vdots & \vdots & \vdots & \vdots & \vdots & \vdots & \vdots & \vdots & \vdots \\ 0 & 0 & 0 & 0 & 0 & 0 & 0 & 0 & 0 & 0 & 0 & 0 \\ \frac{\pm\Phi_{x1}^{(6)}}{M_6\ell\omega_c^2} & \frac{\pm\Phi_{x2}^{(6)}}{M_6\ell\omega_c^2} & \frac{\pm\Phi_{x3}^{(6)}}{M_6\ell\omega_c^2} & \frac{\pm\Phi_{x4}^{(6)}}{M_6\ell\omega_c^2} & 0 & 0 & \frac{\pm\Phi_{x7}^{(6)}}{M_6\ell\omega_c^2} & \frac{\pm\Phi_{x8}^{(6)}}{M_6\ell\omega_c^2} & \frac{\pm\Phi_{x9}^{(6)}}{M_6\ell\omega_c^2} & \frac{\pm\Phi_{x10}^{(6)}}{M_6\ell\omega_c^2} & 0 & 0 \end{bmatrix} \begin{bmatrix} f_{x1} \\ f_{x2} \\ f_{x3} \\ f_{x4} \\ f_{z5} \\ f_{z6} \\ f_{x7} \\ f_{x8} \\ f_{x9} \\ f_{x10} \\ f_{y11} \\ f_{y12} \end{bmatrix} \tag{4}$$

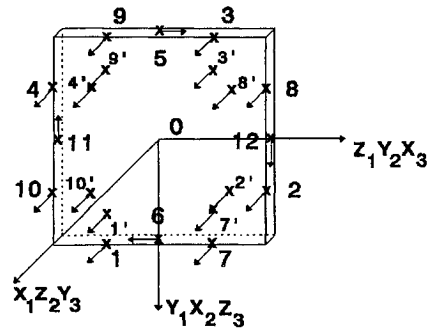

Fig. 1 Sensor/actuator locations, sets full and reduced; primed numbers refer to inner set of actuators and unprimed numbers refer to outer set of actuators.

It is assumed that, for measuring the attitude and displacement of the deformed plate, two Earth horizon sensors, two sun sensors, and γ displacement sensors are to be employed. The Earth sensors measure θ_{e2} and θ_{e3}, the angles between the zenith vector $\hat{i}_0$ ($\hat{j}_0$ is along negative $\dot{\omega}_c$ vector and $\hat{k}_0$ is along velocity vector) and the body axes $\hat{j}$ and $\hat{k}$, respectively. The sun sensors measure θ_{s2} and θ_{s3}, the angles between the direction vector of the sun $\hat{s}_I$, and $\hat{j}$ and $\hat{k}$, respectively. The observational geometrical relationships are

$$\cos\theta_{e2} = \hat{j}\cdot\hat{i}_0 \tag{5a}$$

$$\cos\theta_{e3} = \hat{k}\cdot\hat{i}_0 \tag{5b}$$

$$\cos\theta_{s2} = \hat{j}\cdot\hat{s}_I \tag{6a}$$

$$\cos\theta_{s3} = \hat{k}\cdot\hat{s}_I \tag{6b}$$

From the definition of matrix multiplication and the dot product of a vector

$$\begin{aligned}\hat{i} &= a_{11}\hat{i}_0 + a_{12}\hat{j}_0 + a_{13}\hat{k}_0\\ \hat{j} &= a_{21}\hat{i}_0 + a_{22}\hat{j}_0 + a_{23}\hat{k}_0\\ \hat{k} &= a_{31}\hat{i}_0 + a_{32}\hat{j}_0 + a_{33}\hat{k}_0\end{aligned} \tag{7a}$$

$$\hat{j}\cdot\hat{i}_0 = a_{21}, \qquad \hat{k}\cdot\hat{i}_0 = a_{31} \tag{7b}$$

$$\begin{aligned}\hat{j}\cdot\hat{s}_i &= a_{21}(\hat{i}_0\cdot\hat{s}_i) + a_{22}(\hat{j}_0\cdot\hat{s}_i) + a_{23}(\hat{k}_0\cdot\hat{s}_i)\\ \hat{k}\cdot\hat{s}_i &= a_{31}(\hat{i}_0\cdot\hat{s}_i) + a_{32}(\hat{j}_0\cdot\hat{s}_i) + a_{33}(\hat{k}_0\cdot\hat{s}_i)\end{aligned} \tag{7c}$$

Therefore,

$$\cos\theta_{e2} = a_{21} = -\phi \tag{9a}$$

$$\cos\theta_{e3} = a_{31} = \theta \tag{9b}$$

and

$$\begin{aligned}\cos\theta_{s2} &= a_{21}(\hat{i}_0\cdot\hat{s}_I) + a_{22}(\hat{j}_0\cdot\hat{s}_I) + a_{23}(\hat{k}_0\cdot\hat{s}_I)\\ &= -\phi(\hat{i}_0\cdot\hat{s}_I) + (\hat{j}_0\cdot\hat{s}_I) + \psi(\hat{k}_0\cdot\hat{s}_I)\end{aligned} \tag{10a}$$

$$\begin{aligned}\cos\theta_{s3} &= a_{31}(\hat{i}_0\cdot\hat{s}_I) + a_{32}(\hat{j}_0\cdot\hat{s}_I) + a_{33}(\hat{k}_0\cdot\hat{s}_I)\\ &= \theta(\hat{i}_0\cdot\hat{s}_I) - \psi(\hat{j}_0\cdot\hat{s}_I) + (\hat{k}_0\cdot\hat{s}_I)\end{aligned} \tag{10b}$$

The γ displacement sensors are to be used to measure the plate's transverse (normal to the major surface) displacement parallel to the x axis, i.e.,

$$\begin{aligned}g_i &= C_f U(\xi_i,\beta_i,t)\cdot\hat{i}_b = C_f\sum_j^{\infty}\phi_x^{(j)}(\xi_i,\beta_i)A_j(t)\\ &= C_f\ell\sum_j^{\infty}\phi_x^{(j)}(\xi_i,\beta_i)Z_j(t) \qquad (i=1,2,\ldots,\gamma)\end{aligned} \tag{11}$$

where $U(\xi_i,\beta_i;t)$ is the displacement of the plate at the position point (ξ_i,β_i) and C_f is the coefficient relating the displacement to the output voltage (assume $C_f = 1$).

The state-space observation equation for this system is

$$\{Y\} = [C]\{X\} \tag{12}$$

where $\{Y\}$ is the output vector

$$\{Y\} = \begin{bmatrix}\cos\theta_{e2}\\ \cos\theta_{e3}\\ \cos\theta_{s2} - (\hat{j}_0\cdot\hat{s}_I)\\ \cos\theta_{s3} - (\hat{k}_0\cdot\hat{s}_I)\\ g_1\\ g_2\\ \vdots\\ g_\gamma\end{bmatrix} = \begin{bmatrix}-\phi\\ \theta\\ -\phi(\hat{i}_0\cdot\hat{s}_I) + \psi(\hat{k}_0\cdot\hat{s}_I)\\ \theta(\hat{i}_0\cdot\hat{s}_I) - \psi(\hat{j}_0\cdot\hat{s}_I)\\ g_1\\ g_2\\ \vdots\\ g_\gamma\end{bmatrix} \tag{13}$$

and $[C]$ is the observation matrix

$$[C] = \begin{bmatrix}\begin{bmatrix}0 & 0 & 0 & 0 & -1 & 0\\ 0 & \vdots & 1 & \vdots & 0 & \vdots\\ (\hat{k}_0\cdot\hat{s}_I) & \vdots & 0 & \vdots & -(\hat{i}_0\cdot\hat{s}_I) & \vdots\\ -(\hat{j}_0\cdot\hat{s}_I) & 0 & (\hat{i}_0\cdot\hat{s}_I) & 0 & 0 & 0\end{bmatrix}\\ O_{\gamma\times 6}\end{bmatrix}$$

$$\begin{bmatrix}O_{4\times 12}\\ C_f\ell\begin{bmatrix}\phi_{x1}^{(1)} & 0 & \phi_{x1}^{(2)} & 0 & \cdots & \phi_{x1}^{(6)} & 0\\ \phi_{x2}^{(1)} & 0 & \phi_{x2}^{(2)} & 0 & \cdots & \phi_x^{(6)} & 0\\ \vdots & \vdots & \vdots & \vdots & \cdots & \vdots & \vdots\\ \phi_{x\gamma}^{(1)} & 0 & \phi_{x\gamma}^{(2)} & 0 & \cdots & \phi_{x\gamma}^{(6)} & 0\end{bmatrix}_{\gamma\times 12}\end{bmatrix}_{(4+\gamma)\times 18} \tag{14}$$

After application of the small angle approximation for $\theta \ll 1$, $\sin\theta \approx \theta$, and $\cos\theta \approx 1$, to the transformation matrix (from the body frame to the orbit frame), T_{b0} becomes

$$T_{b0} \approx \begin{bmatrix}1 & \phi & -\theta\\ -\phi & 1 & \psi\\ \theta & -\psi & 1\end{bmatrix} = \begin{bmatrix}a_{11} & a_{12} & a_{13}\\ a_{21} & a_{22} & a_{23}\\ a_{31} & a_{32} & a_{33}\end{bmatrix} \tag{8}$$

The various dot product terms in $[C]$ become

$$\begin{bmatrix}\hat{i}_0\cdot\hat{s}\\ \hat{j}_0\cdot\hat{s}\\ \hat{k}_0\cdot\hat{s}\end{bmatrix} = [A_{0I}]\cdot[\hat{s}^I] = [A_{0I}]\cdot\begin{bmatrix}\cos\delta_s\cos\alpha_s\\ \cos\delta_s\sin\alpha_s\\ \sin\delta_s\end{bmatrix} \tag{15}$$

$$\begin{bmatrix} \hat{i}_0 \cdot \hat{s} \\ \hat{j}_0 \cdot \hat{s} \\ \hat{k}_0 \cdot \hat{s} \end{bmatrix} = \begin{bmatrix} C\delta_s C\alpha_s (C\Omega C(\omega+f) - S\Omega S(\omega+f)C\iota) + C\delta_s S\alpha_s (S\Omega C(\omega+f) + C\Omega S(\omega+f)C\iota) + S\delta_s S\iota S(\omega+f) \\ -(C\delta_s C\alpha_s S\Omega S\iota) + C\delta_s S\alpha_s C\Omega S\iota - (S\delta_s C\iota) \\ -C\delta_s C\alpha_s (C\Omega S(\omega+f) + S\Omega C(\omega+f)C\iota) + C\delta_s S\alpha_s (-S\Omega S(\omega+f) + C\Omega C(\omega+f)C\iota) + S\delta_s S\iota C(\omega+f) \end{bmatrix} \tag{16}$$

From the STS-57 mission, the necessary Keplerian values for populating the observation matrix are orbital inclination $\iota = 28.4595°$, right ascension of the node $\Omega = 251.4830°$, argument of the perigee $\omega = 96.9871°$, and mean anomaly $f = 263.7718°$. The mission flight date was June 30, 1993; from Ref. 12 the angles obtained for the sun position vector are listed as follows: apparent declination of the sun $\delta_s = 23°11'$ and right ascension of the sun $\alpha_s = 98°13'$ (example assumes constant mean anomaly). With the substitution of these angular values, the dot products become

$$\begin{bmatrix} \hat{i}_0 \cdot \hat{s} \\ \hat{j}_0 \cdot \hat{s} \\ \hat{k}_0 \cdot \hat{s} \end{bmatrix} = \begin{bmatrix} -0.82177 \\ -0.54057 \\ -0.17117 \end{bmatrix} \tag{17}$$

Application of SVD Transformation

Through the comparison of the singular values of the system transfer function one arrives at suitable ranges for stability robustness. Throughout this research, singular value plots are utilized for the analysis of the various systems. It was noted that the system singular values were close to zero. To alleviate this problem with singularity, the SVD method was applied to transform the original systems. The number of removed controller/observer components corresponds to the number of controller/observer matrix singular values close to zero. (The reduction of actuators/sensors is done partially in the physical sense and partially in the mathematical space.)

Initially, simulations were run for systems 1–4 to obtain transient time responses for different values of measurement noise parameter μ and the weighting parameter ρ. The measurement noise covariance matrix R is $E\{(\mu I^n(k))(\mu I^n(k))^T\} = \mu^2 \times [I] = R$. The control penalty matrix $\hat{R}$ is $\hat{R} = \rho^2 \times [I]$. Then, once reasonable responses were acquired through dynamic simulation, an attempt was made to obtain the singular value frequency plots. Unfortunately, the system's open-loop singular values were extremely close to zero, denoting a lack of linear independence in some (if not all) of the system's matrices. A review of the definition of a singular matrix follows[9,13]: 1) some rows are linearly dependent, 2) the inverse of the matrix may not exist, 3) its determinant is equal to zero, and 4) zero is a possible eigenvalue of the matrix. Because all of these properties existed, here a singular value decomposition transformation method was applied to remove some of the linear dependent rows. The steps are as follows:

$$\dot{x} = Ax + Bu, \qquad y = Cx \tag{18}$$

$$C = U\Sigma V^T \tag{19}$$

where

$$\Sigma = \begin{bmatrix} \sigma_{(n-m)\times(n-m)} & 0 \\ 0 & 0_{m\times m} \end{bmatrix}$$

is the diagonalized matrix containing the singular values of C. Now C becomes

$$C \to C = [\sigma]_{(n-m)\times(n-m)} \tag{20}$$

where m is the number of zero singular values

$$y = U\Sigma V^T x \Rightarrow U^T y = \Sigma V^T x \tag{21}$$

Define

$$\hat{x} = V^T x, \qquad \hat{y} = U^T y \tag{22}$$

Given $\hat{x}$ and $\hat{y}$, one can always recover x and y from

$$x = V\hat{x}, \qquad y = U\hat{y} \tag{23}$$

Therefore, the state and output equations become

$$\dot{\hat{x}} = \hat{A}\hat{x} + V^T Bu, \qquad \hat{y} = \hat{C}\hat{x} \tag{24}$$

where

$$\hat{A} = V^T A V, \qquad \hat{C} = \Sigma$$

Next let

$$B = \tilde{U}\tilde{\Sigma}\tilde{V}^T \tag{25}$$

where

$$\tilde{\Sigma} = \begin{bmatrix} \tilde{\sigma}_{(r-s)\times(r-s)} & 0 \\ 0 & 0_{s\times s} \end{bmatrix}$$

is the diagonalized matrix containing the singular values of B and where s is the number of zero singular values. Note

$$V^T Bu = (V^T\tilde{U})\tilde{\Sigma}(\tilde{V}^T u) = \tilde{B}\tilde{\Sigma}\hat{u} = \hat{B}\hat{u} \tag{26}$$

where

$$\tilde{B} = V^T\tilde{U}, \qquad \hat{B} = \tilde{B}\tilde{\Sigma}, \qquad \hat{u} = \tilde{V}^T u$$

The state and output equations become

$$\dot{\hat{x}} = \hat{A}\hat{x} + \hat{B}\hat{u}, \qquad \hat{y} = \hat{C}\hat{x} \tag{27}$$

Note the corresponding penalty matrices are

$$Q = BB^T \Rightarrow Q = V^T\tilde{U}\tilde{\Sigma}\tilde{\Sigma}^T\tilde{U}^T V, \qquad R = \rho^2 I$$
$$\hat{Q} = C^T C \Rightarrow Q = \Sigma^T\Sigma, \qquad \hat{R} = \mu^2 I \tag{28}$$

After the system is transformed, the eigenvalues for the system were recalculated. It was found that these values were exactly the same for the untransformed and transformed systems. Examples of the maximum and minimum singular value plots for the transfer matrices of the original and the SVD transformed systems are shown in Figs. 2–5.

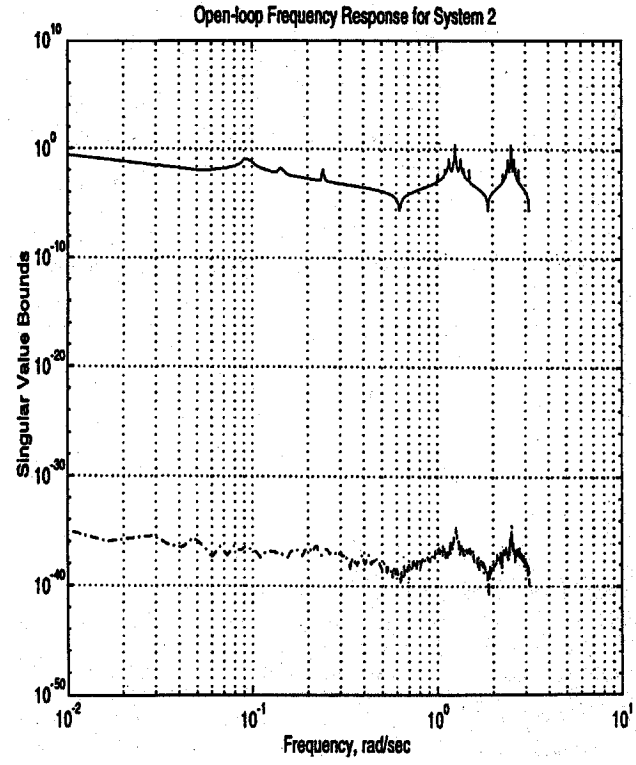

Fig. 2 Open-loop singular value for system 2.

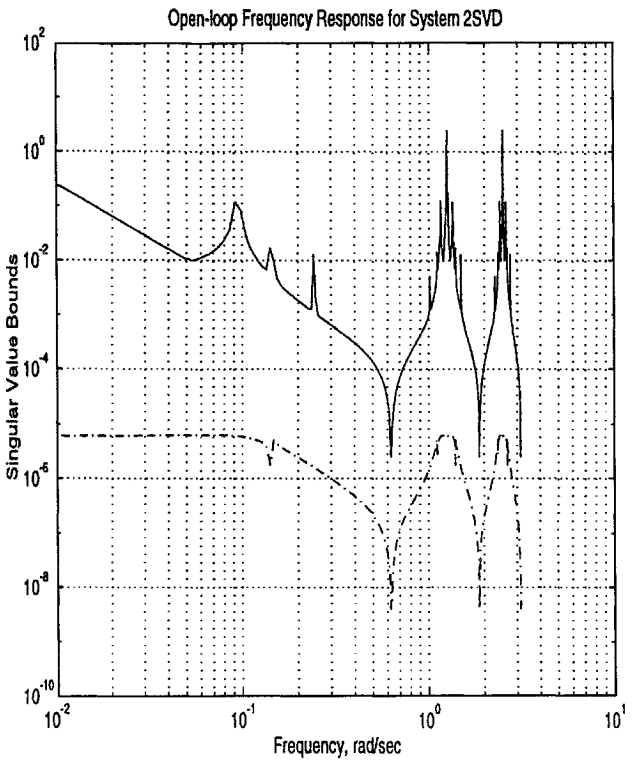

Fig. 3 Open-loop singular value for system 2 SVD.

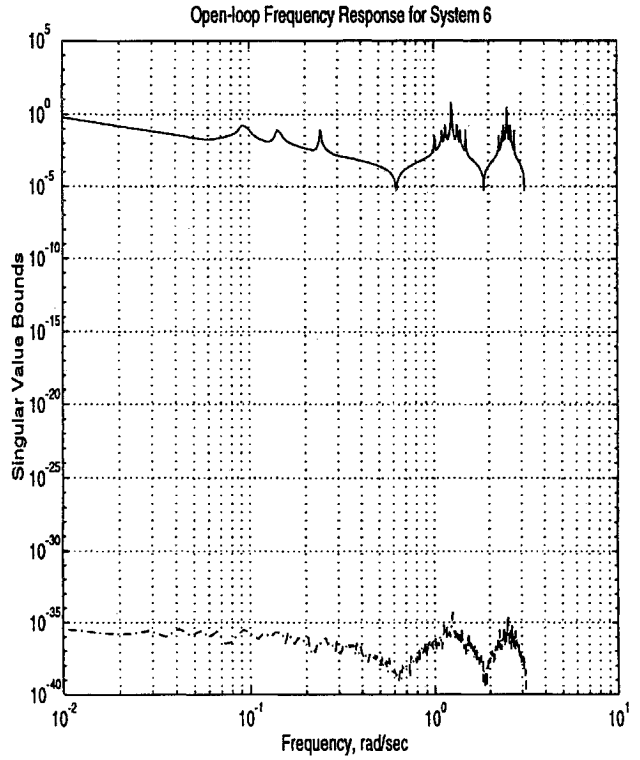

Fig. 4 Open-loop singular value for system 6.

These figures represent the open-loop transfer function singular value bounds plots before and after an SVD transformation is applied to the system.[13] Note that the closer the singular value is to zero, the closer the system is to singularity. When comparing the singular value bounds for the untransformed and transformed systems, one notices a difference in the minimum singular values. The (transformed) singular value bounds are reduced and the minimum singular values are increased; therefore, an improvement has been made by reducing the number of linearly dependent rows in the original system matrices.

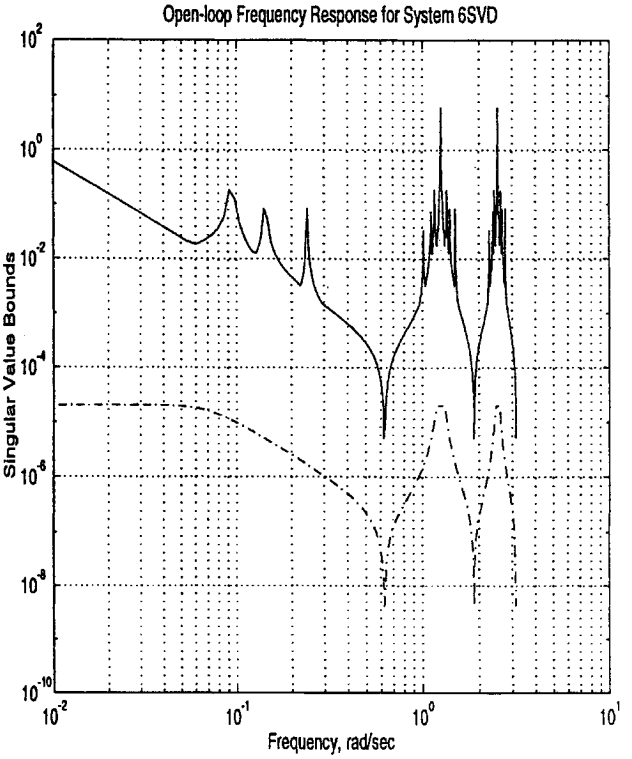

Fig. 5 Open-loop singular value for system 6 SVD.

Discussion of Results

The increase in the minimum singular value from the original system to the SVD transformed system for systems 1, 2, and 6 is much larger than for systems 3–5. This dramatic difference corresponds to systems 1, 2, and 6 being full order, thus, reflecting the possibility of more redundant variables than the reduced order of systems 3–5. After the use of the SVD transformation, the minimum singular value for system 1 increases from 10^{-40} to 10^{-16}, and systems 2 and 6 increase from 10^{-40} to 10^{-8}. The differences in the change in the minimum singular values for the three systems (1, 2, and 6) are because system 1 utilizes an all outer actuator placement, system 2 demonstrates an all inner actuator placement, and system 6 incorporates a combined inner and outer actuator placement. From the results, it appears that system 2 and 6 have less tendency toward singularity problems than system 1. Noting that both of these systems, 2 and 6, involve inner actuator placement, it is possible that the use of inner placement creates a less redundant system. When comparing the reduced-order systems 3–5, one immediately notices that the minimum singular value for systems 3 and 4 increases from 10^{-22} to 10^{-20} and system 5 with a minimum singular value of 10^{-8} does not appear to change after the SVD transformation. These systems do not exhibit much change because these systems are already reduced systems, and so there is less chance of redundancy in the variables. In the case of system 5, this system is already so low ordered (three rigid-body modes and two generic modes) that there is an even smaller chance of redundancy.

After the system is transformed, the eigenvalues for the system, as well as the degree of controllability and observability, for the system were recalculated. These characteristic system values were the same for the untransformed and transformed systems. The LQG transient time responses for these same systems are displayed as verification of their improved performance. There is a significant change in the systems' performance when the bound is reduced. Of course, the change is not as drastic in the smaller reduction of singular value bounds, i.e., 10^{-40}–10^{-18}, but in the case of the larger reduction in singular value bounds, i.e, 10^{-40}–10^{-8}, is more noticeable. Examples are provided in Figs. 6–11. Initial conditions assume the rigid-body modes experience a 1% deflection, i.e., $x_0(1, 3, 5) = 0.01$, all other state variables are initially equal to zero.

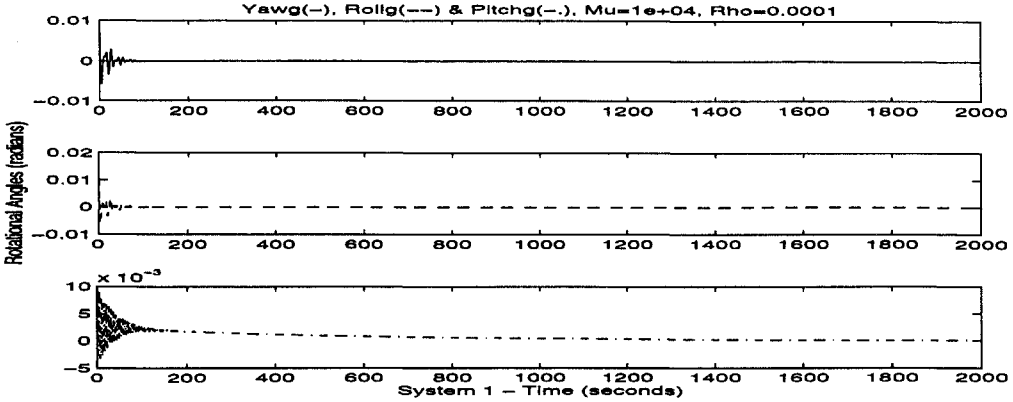

Fig. 6 Yaw, roll, and pitch for system 1; $\rho = 1 \times 10^{-4}$, and $\mu = 1 \times 10^{4}$.

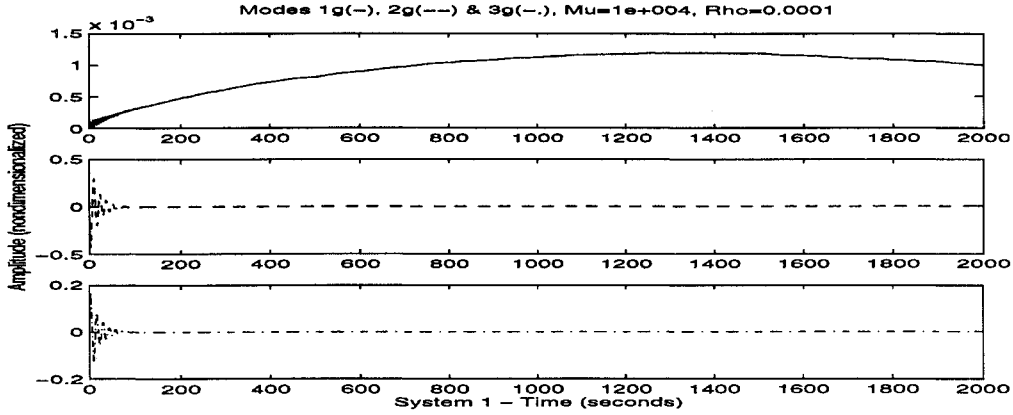

Fig. 7 Modes 1–3 for system 1; $\rho = 1 \times 10^{-4}$, and $\mu = 1 \times 10^{4}$.

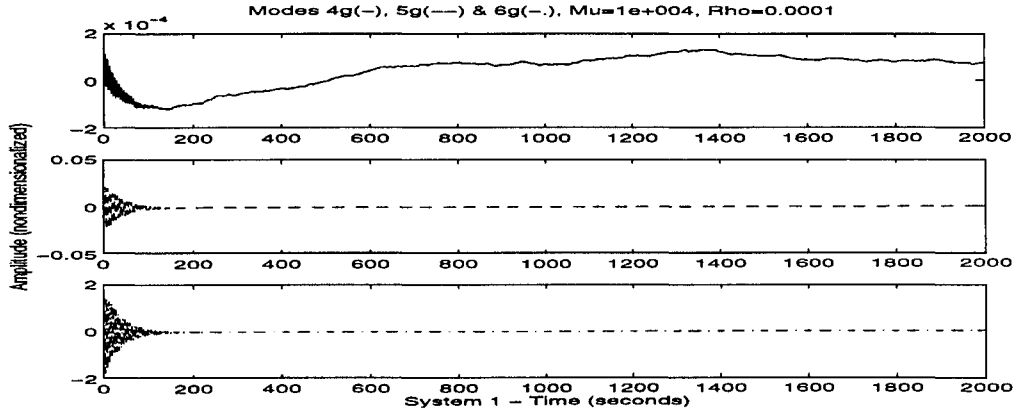

Fig. 8 Modes 4–6 for system 1; $\rho = 1 \times 10^{-4}$, and $\mu = 1 \times 10^{4}$.

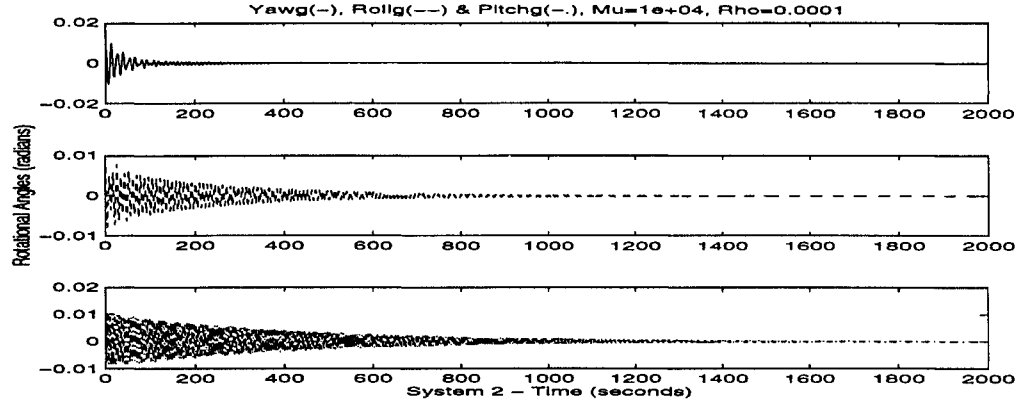

Fig. 9 Yaw, roll, and pitch for system 2; $\rho = 1 \times 10^{-4}$, and $\mu = 1 \times 10^{4}$.

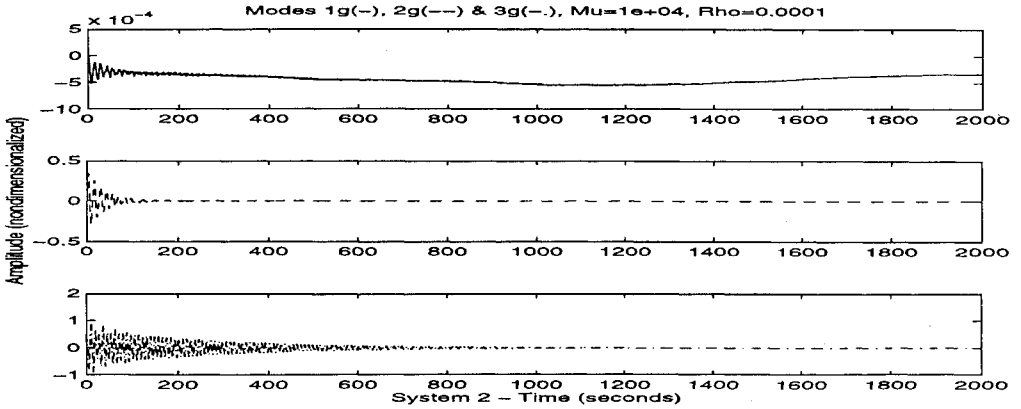

Fig. 10 Modes 1–3 for system 2; $\rho = 1 \times 10^{-4}$, and $\mu = 1 \times 10^{4}$.

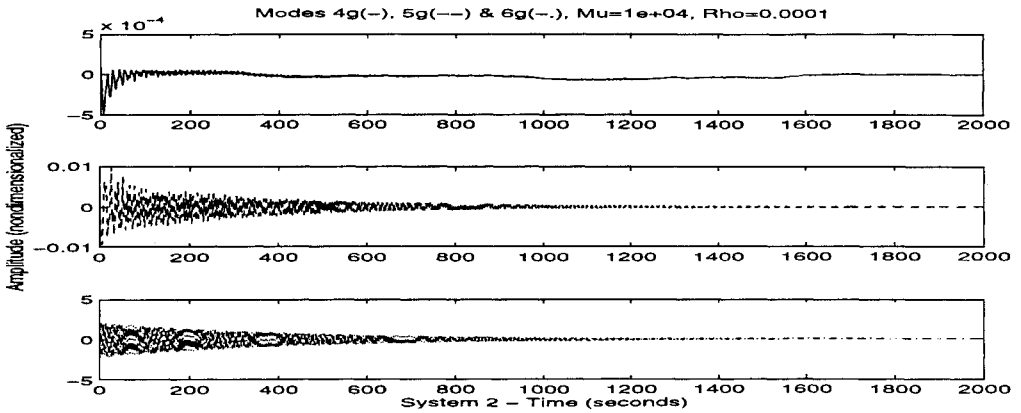

Fig. 11 Modes 4–6 for system 2; $\rho = 1 \times 10^{-4}$, and $\mu = 1 \times 10^{4}$.

Conclusions

Singular value plots are utilized for analysis of the various systems throughout this research. It was noted that the singular values of the open-loop system transfer function were extremely close to zero. These singularities in the system represent redundancies in the system modeling, in this case, caused by the symmetrical arrangements of the actuators/sensors with respect to the nodal (repetitive) patterns of the homogeneous square plate. To alleviate the problem with singularities, the SVD method was applied to transform the original systems to a nonredundant controller/observer system. When comparing the singular value bounds for the untransformed and transformed systems, one notices a difference in the minimum singular values. The (transformed) singular value bounds are reduced and the minimum singular values are increased; therefore, an improvement has been made by reducing the number of redundant actuators and sensors in the system.

The increase in the minimum singular value from the original system to the SVD transformed system is much larger for the full-ordered state space systems than for the reduced-ordered state-space systems. This dramatic difference reflects the presence of more redundant variables in the full-ordered state-space system than in the reduced ordered state-space systems. From the results, it appears that systems utilizing the interior placement of the actuators/sensors result in fewer singularities than the systems based on outer (exterior) arrangement of actuators/sensors. This suggests the possibility that the use of inner placement results in a more uniform controller/observer system with less redundancies in actuator/sensor modeling. Overall the use of the SVD transform method produces a vast improvement in the bounds of the singular value.

Acknowledgment

Support was supplied by a Howard University/NASA Grant for the Center for Study of Extraterrestrial and Terrestrial Atmospheres.

References

[1]Santini, P., "Stability of Flexible Spacecrafts," *Acta Astronautica*, Vol. 3, Sept.–Oct. 1976, pp. 685–713.

[2]Friedland, B., *Control System Design—An Introduction to State-Space Methods*, McGraw–Hill, New York, 1986, pp. 15–57.

[3]Schaeffer, H. G., *MSC/NASTRAN Primer: Static and Normal Mode Analysis*, Schaeffer Analysis, Mount Vernon, NH, 1979.

[4]Tan, Z., and Bainum, P. M., "The Optimal LQG Digital Control of an Orbiting Large Flexible Platform," *Proceedings of International Conference on Dynamics, Vibration and Control* (Beijing, PRC), Peking Univ. Press, 1990, pp. 179–193.

[5]Xing, G., and Bainum, P. M., "Actuator Placement Using Degree of Controllability for Discrete-Time Systems," *Transactions of the ASME*, Vol. 114, Sept. 1992, pp. 508–516.

[6]Ericsson-Jackson, A. J., Bainum, P. M., and Xing, G., "Actuator/Sensor Placement Using Degree of Controllability and Observability for Digitally Controlled Orbiting Platforms," *Journal of the Astronautical Sciences*, Vol. 45, No. 1, 1997, pp. 73–89.

[7]Doyle, J. C., and Stein, G., "Multivariable Feedback Design: Concepts for a Classical/Modern Synthesis," *IEEE Transactions on Automatic Control*, Vol. AC-26, No. 1, 1981, pp. 4–17.

[8]Stein, G., and Athans, M., "The LQG/LTR Procedure for Multivariable Feedback Control Design," *IEEE Transactions on Automatic Control*, Vol. AC-32, No. 2, 1987, pp. 105–114.

[9]Golub, G. H., and Riensch, C., "Singular Value Decomposition," *Handbook for Automatic Computation: Linear Algebra*, edited by J. H. Wilkinson, C. Reinsch, and F. L. Bauer, Vol. 2, Springer–Verlag, Berlin, 1971, pp. 134–152.

[10]*Matlab: User's Guide*, MathWorks, South Natick, MA, May 1989.

[11]Yu, E. Y., "Long-Term Coupling Effects between Librational and Orbital Motions of a Satellite," *AIAA Journal*, Vol. 2, No. 3, 1964, pp. 553–555.

[12]*Astronomical Almanac of 1993*, National Almanac Office, U.S. Naval Observatory, U.S. Government Printing Office, Science and Engineering Research Council, Washington, DC, 1992, p. C10.

[13]Ericsson-Jackson, A. J., "The Robust Digital Control of a Large Orbiting Space Structure," Ph.D. Dissertation, Dept. of Mechanical Engineering, Howard Univ., Washington, DC, July 1995.